12-1-2023

LEW.WR1 Rats Develop Non-Alcoholic Steatohepatitis: Does FAT10 Play a Role in Steatosis Development

Christopher Riley Apperson

Follow this and additional works at: https://louis.uah.edu/honors-capstones

LEW1.WR1 Rats Develop Non-Alcoholic Steatohepatitis: Does FAT10 play a role in steatosis development?
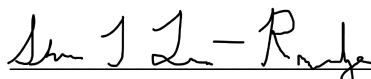
by

Christopher Riley Apperson

An Honors Capstone
submitted in partial fulfillment of the requirements
for the Honors Diploma
to
The Honors College
of
The University of Alabama in Huntsville
12/1/23

Honors Capstone Project Director: Dr. Sharifa Love-Rutledge

_____ 12/1/23
Student (signature)   Date

_____ 12/1/23
Project Director (signature)   Date

_____ 12/1/2023
Department Chair (signature)   Date

_____
Honors College Dean (signature)   Date

Honors Thesis Copyright Permission

This form must be signed by the student and submitted with the final manuscript.

In presenting this thesis in partial fulfillment of the requirements for Honors Diploma or Certificate from The University of Alabama in Huntsville, I agree that the Library of this University shall make it freely available for inspection. I further agree that permission for extensive copying for scholarly purposes may be granted by my advisor or, in his/her absence, by the Chair of the Department, Director of the Program, or the Dean of the Honors College. It is also understood that due recognition shall be given to me and to The University of Alabama in Huntsville in any scholarly use which may be made of any material in this thesis.

Christopher Riley Apperson
_____

Student Name (printed)

_____

Student Signature

12/1/23
_____

Date

LEW1.WR1 Rats Develop Non-Alcoholic Steatohepatitis: Does FAT10 play a role in steatosis development?

Abstract

Despite the prevalence of fatty liver conditions in humans, understanding the mechanisms behind these conditions still leaves much to be desired. Recent work has demonstrated that the LEW1.WR1 rat breed serves as a reliable animal model for fatty liver diseases, allowing for diet regulation, in-depth sequencing, and post-mortem studies. The development of fatty infiltrates of the liver in this model opened these rats to further studies on the pathophysiological causes of fatty liver. We perceive that this is connected to the increased FAT10 gene expression, a gene identified in human studies of fatty liver disease. We assessed liver microvesicular steatosis, Mallory Denk body formation, inflammatory body formation, and lipid accumulation to quantify the disease status. To further assess the role of FAT10 in hepatocytes, an *in vitro* model was also evaluated for the development of increased lipid stores. Upregulation of FAT10 was confirmed via qPCR. In total, higher FAT10 activity has been connected to cellular pathology of fatty liver disorders.

Introduction

A growing medical issue worldwide is the prevalence of non-alcoholic fatty liver disease (NAFLD), which is linked to several different pathologies, including accumulation of fatty acids and triglycerides[3]. NAFLD is particularly associated with type II diabetes and cardiovascular conditions, given its accumulation of lipids in not only the liver, but also other organs and along body cavity linings[1]. This build-up of lipids within hepatocytes induces cellular strain and inflammation, and this gradually causes damage to the liver. Further progression of NAFLD results in an advanced condition known as non-alcoholic steatohepatitis (NASH)[4]. This disease progression itself has not been rigorously tested; however, the current understanding suggests that increased inflammation in NAFLD leads to NASH, and this is coupled with steatosis[5]. Advanced NASH then results in liver damage, up to and including fibrosis, ballooning, and cirrhosis[3,5]. The general pathological characteristics of NAFLD/NASH, as deduced from liver biopsies, include ballooning, fibrosis, inflammation, and steatosis[3].

Prior *in vivo* studies used live rats to model NAFLD/NASH in humans. In particular, LEW1.WR1 (1WR1) rats were compared against Wistar-Furth (WF) along the known metrics of these diseases; i.e., fat mass and liver cell markers. The former group has been shown to exhibit susceptibility for the induction of type 1 diabetes-like symptoms, especially with respect to the nonsusceptible WF model[2]. Harvesting and weighing of visceral abdominal fat showed that 1WR1 rats develop increased body mass and liver mass even under a controlled diet with normal levels of sucrose and fat[4]. It was unclear from mass alone what effects this had on a cellular level, necessitating further histological analysis.

Similarly, genetic studies on the 1WR1 model showed increased expression of the FAT10 gene in the NAFLD/NASH conditions[4]. However, this again gave no indication of hepatocytic effects; the suggestion was that the observed uptick in lipid storage was only correlated with the upregulation of FAT10.

Given the prior study, these experiments investigated this increased steatosis and inflammation in the fatty 1WR1 rats, compared to WF, in an effort to find a positive correlation. Histological slices of the rats' livers, previously harvested and scanned, were examined at a cellular level. Standardized counts of several pathological markers were used to quantitate cellular damage and lipid retention between the two groups. Furthermore, these experiments sought to explore the link between FAT10 expression and hepatocyte lipid accumulation. Where Wimalarathne et al. implied FAT10 upregulation as a result of NASH/NAFLD, here the gene expression was first increased via viral transduction, and the cells are evaluated for evidence of steatosis. Oil Red O (ORO) staining with fluorescent imaging qualifies the greater presence of lipid droplets in experimental hepatocytes compared to controls, while qPCR confirms the higher activity of FAT10 in the same cells. If FAT10 is a cause of steatosis and NAFLD/NASH effects, then this upregulation of FAT10 should result in higher lipid accumulation, indicated by ORO stain and quantified through UV-vis absorbance.

Materials and Methods

Rats:

The 11 male LEW.1WR1 (1WR1) rats arrived from Bio mere (Worcester, MA) (one rat developed type 1 diabetes and was removed from the study). The 8 Wistar Furth (WF/NH's) rats arrived from Envigo (Indianapolis, IN). Rats were 2 to 3 weeks old upon arrival. The animals were maintained with a 12-hour

light-dark cycle. During the acclimation period, the animals were given water and a standard Envigo chow diet ad libitum with access to enrichment. The animals were randomized in groups of 3 and 4 per cage and were acclimated to the environment a week before testing began. Both rat groups were put on a control diet (LFD: D12450k Research Diets, New Brunswick, NJ) at age of week 5 or beginning of the experiment.

The length of the entire study was 18 weeks; thus the rats were 20-21 weeks old by the end. The experimental protocol was approved by the University of Alabama in Huntsville Institutional Animal Care and Use Committee.

Rats were anesthetized, and exsanguinated, the liver was dissected out of the abdominal cavity and weighed. The left medial lobe was then dissected away, placed in a cassette and placed in Neutral buffered formalin (10%) (Thermo Fisher Scientific) for 24 hours for fixing. After fixing, the organ was placed in 70% Ethanol (Thermo Fisher Scientific) and mailed to Histowiz (Brooklyn, New York). Histowiz paraffin embedded, sectioned (4 μm), and stained the slides with Hematoxylin and Eosin and Trichrome blue stain.

Pathological analysis :

Mallory Denk body formation was scored as 0: not present, 1: present. The presence of microvascular and macrovascular steatosis was evaluated in five randomly chosen rectangular areas of 0.3 mm2 at fields of 40× magnification in areas with steatosis and scored as 0: not present, 1: present.

Microvesicular Steatosis and Mallory Denk Body Scoring:

Two images were taken of each of sixteen mouse liver slides, one from the center of the slide and one from the edge. Each image was scored for microvesicular steatosis as either 1 or 0, indicating present or not. Mallory Denk bodies were similarly evaluated using one image per slide.

Cells:

Hepatocytes used for *in vitro* experiments included ATCC FL83B cells cultured in F12K + 10% FBS media and harvested at passage number 5. These were thawed from liquid nitrogen and maintained in a T75 flask with 15-20 mL of media and 30-40 μL of plasmocin prior to plating and later harvesting.

Oil Red O Experiment:

Hepatocytes were cultured to 90% confluency with F12K + 10% FBS media in a T75 flask. These were counted and 100,000 cells were plated in each of 10 MatTek 35mm No. 1.5 dishes. A viral media was made with F12K +1% FBS and a lentivirus that upregulated FAT10, pLV[Exp]-EGFP:T2A:Puro-EF1A>mUbd[NM_023137.3] (VB900008-4117cfb), from VectorBuilder. The cells were then infected with the viral media. The virus was allowed to propagate for at least 3 days, checking for progress via fluorescence of the cells, before finally proceeding on day 5. Novolin R insulin (100 units/mL) was added to induce steatosis and the media was removed. The cells were then washed with phosphate-buffered saline (PBS) and fixed in 2 mL each of 10% formalin for 1 hour at room temperature. These were washed with DI water to remove the formalin, followed by 2 mL of 60% isopropanol for 5 minutes. A stock Oil Red O (ORO) solution was prepared with 300 mg Oil Red O powder (catalog no. O0625; Sigma-Aldrich) dissolved in 100 mL 99% isopropanol. A working ORO solution was prepared with 3 parts ORO stock to 2 parts DI water. The cells were stained with 2 mL ORO working solution in order to create red markers in the presence of lipid droplets, left for 5 minutes at room temperature, and rinsed with DI water until clear. The droplets were imaged in both transmitted and fluorescent light. The lipids were then dissolved in isopropanol before taking UV-vis absorbance measurements at 515 nm via a spectrophotometer.

Using unfixed hepatocytes remaining in the flask, their media was removed and 100 μL of Trizol was added for 2 minutes to begin extracting their RNA. These were pipetted out and centrifuged before adding 700 μL of Trizol reagent. 200 μL chloroform was added and the cells were vortexed and centrifuged, isolating the aqueous RNA from the proteins and lipids. To precipitate the RNA, 500 μL of isopropanol was added before vortexing and centrifugation. The RNA was washed with 1 mL 75% ethanol, again vortexed and centrifuged, and finally dried with a Savant vacuum. This RNA, redissolved in 20 μL nuclease-free water, was quantified via a NanoDrop 2000c spectrophotometer. It was converted to stable cDNA through RT-PCR and expression of the UBD gene (FAT10) was evaluated via qPCR. The RPL32 gene was measured alongside as a housekeeping gene. SYBR Green Master Mix was used to dye and quantify the RNA. The primers used for these genes were:

- RPL32 forward: aaactggcggaaacccagag

- RPL32 reverse: gcaatctcagcacagtaagatt

- UBD forward: gagtccaaaaacgaggggca

- UBD reverse: ttccagcttcttttccgttgc

The cell culturing, viral infection, fixation, and harvesting was repeated with a control lentivirus, likewise from VectorBuilder, pLV[Exp]-EGFP:T2A:Puro-EF1A>mCherry (VB010000-9298rtf).

Results

As shown in Figure 1 of Results, the 1WR1 rat model was positively correlated with higher instances of microvesicular steatosis in the liver, according to its use as a NAFLD/NASH human analog. Figures 2 and 3, demonstrating cellular damage and inflammation respectively, further confirmed this connection. However, it was unclear by this point whether the disease effected these conditions or the two were simply correlated. In order to assess this as a causative relationship, studies were shifted to *in vitro*, first evaluating gene expression of the 1WR1 rats. The FAT10 gene was consistently upregulated in this group, confirming a genetic basis for the conditions. Next, mouse FL83B hepatocytes were infected with a lentivirus that upregulated FAT10, before a high-insulin treatment, mimicking a diabetes-like state. Those cells, in comparison to cells infected with a control virus, had noticeably higher average levels of lipid retention, as seen in Figures 4 and 5
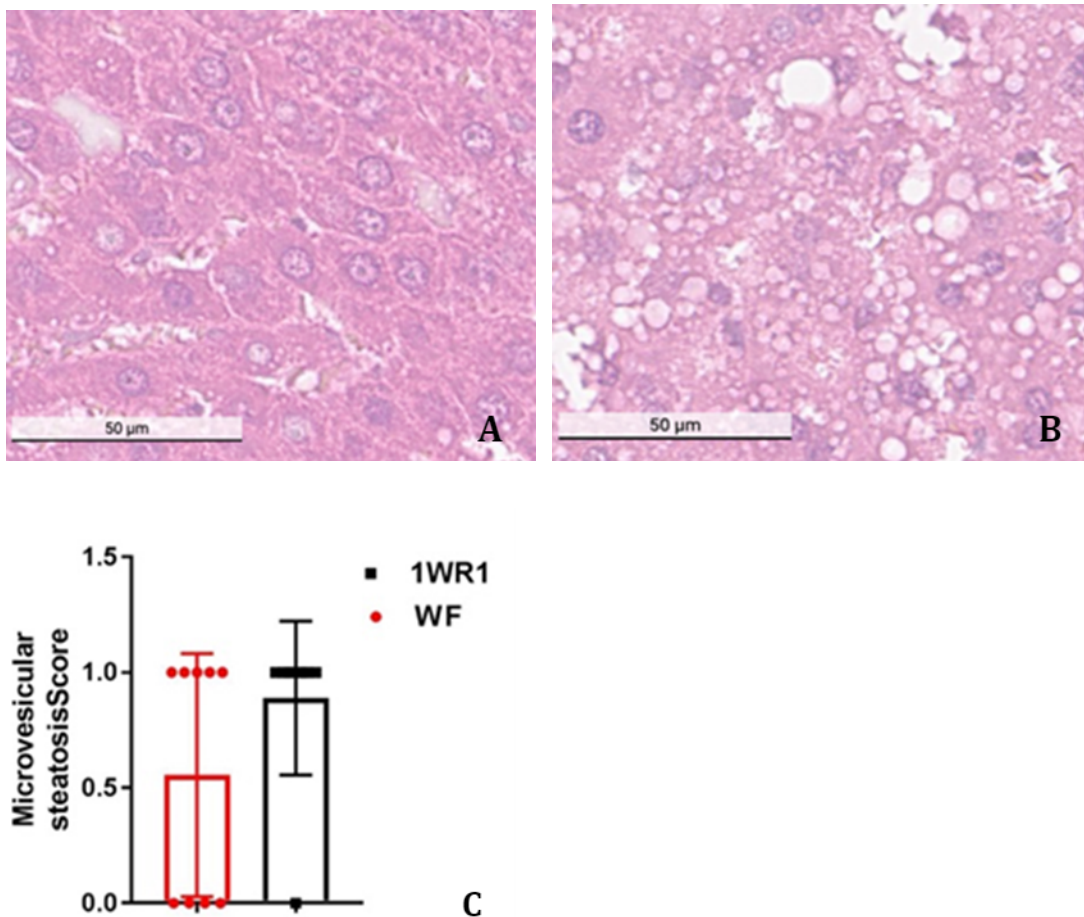

Figure 1: LEW1.WR1 rats have higher counts of microvesicular steatosis. WF rats (A) have visibly less steatosis in hepatocytes than do 1WR1 rats (B). The lipid droplets are visualized as white, circular inclusions around many nuclei in (B). This is quantified via a scoring metric and unpaired t-test in (C)[3].
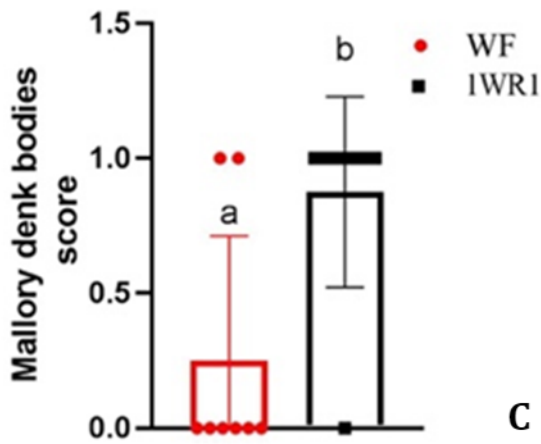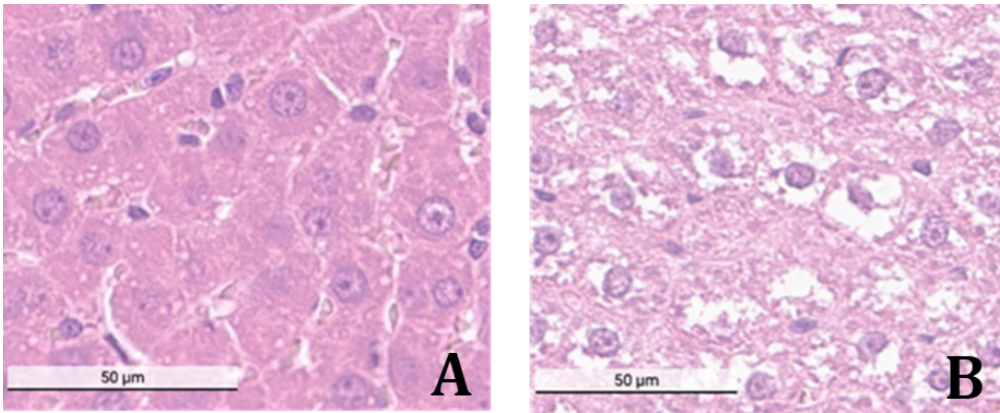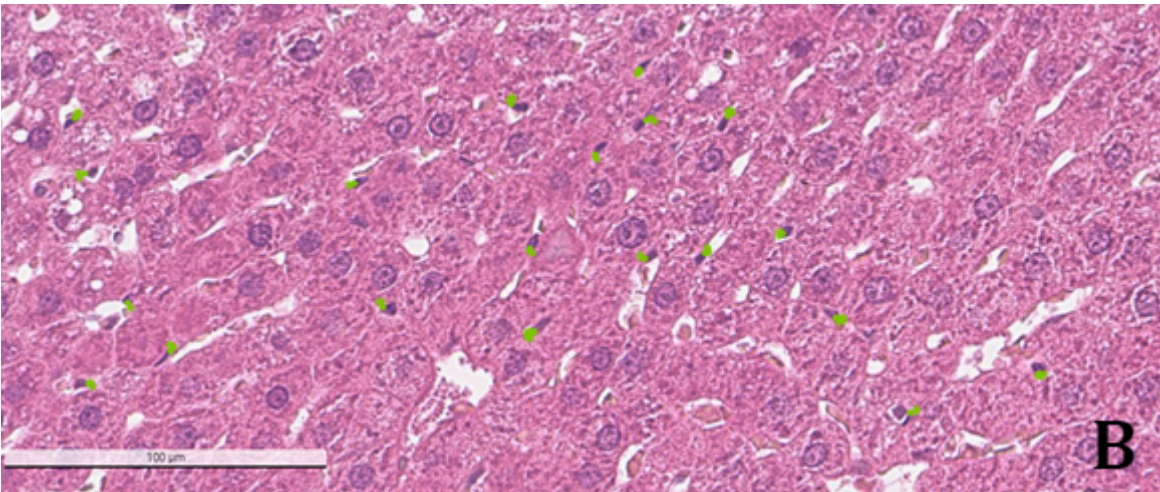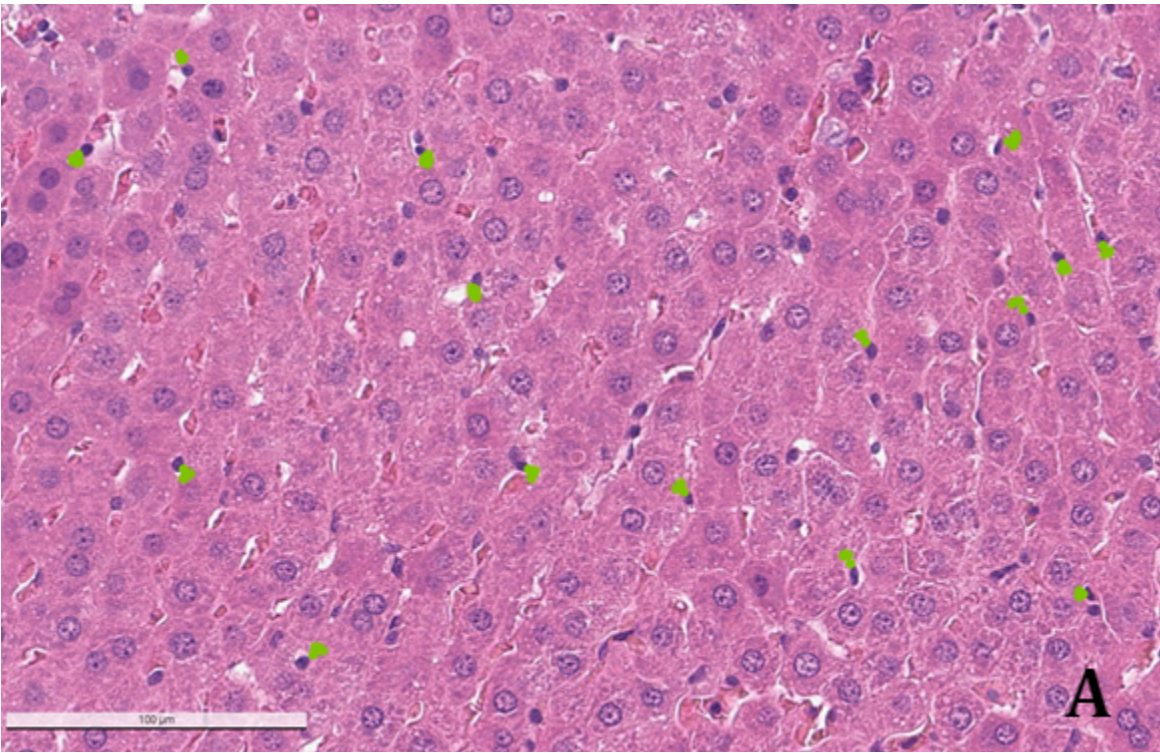
Figure 2: LEW1.WR1 rats have Mallory Denk (MD) body formation. WF rat hepatocytes show little to no MD body formation (A), compared to those in 1WR1 hepatocytes (B). The MD bodies are seen as light purple filaments around the nuclei in (B). The unpaired t-test (C), taken from Wimalarathne et al., quantifies this.
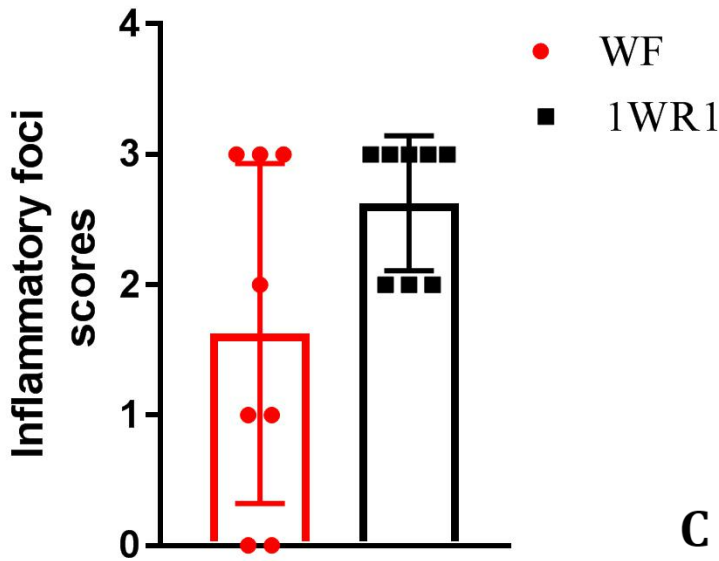
Figure 3: LEW1.WR1 rats have higher inflammatory scores. Between WF hepatocytes (A) and 1WR1 hepatocytes (B), the latter show markedly more inflammatory bodies. These are seen as irregular, dark-purple spots, highlighted with green marks above and distinguished from nuclei. An unpaired t-test (C) confirms the inflammatory scores of the two different mice groups relative to each other, with standard deviation as the error bars[2].
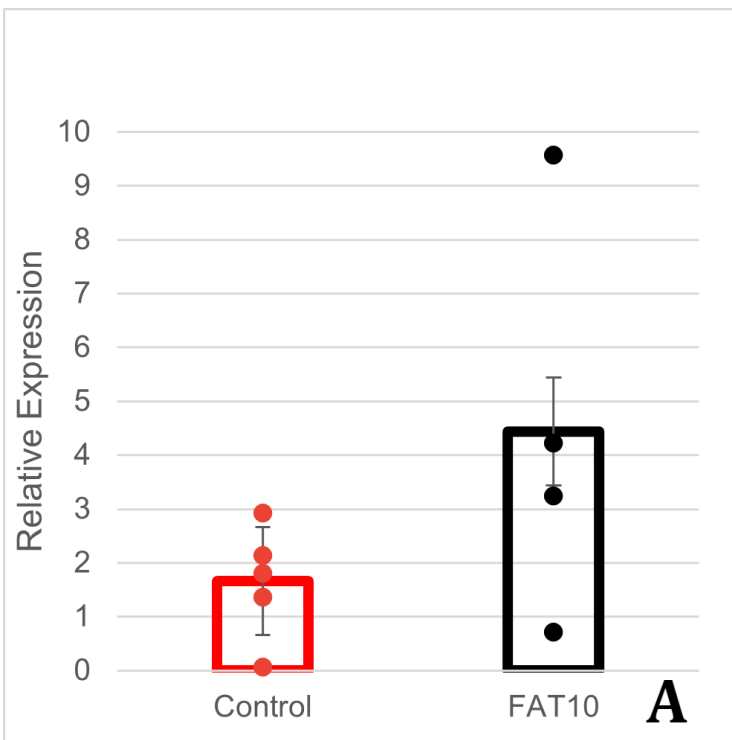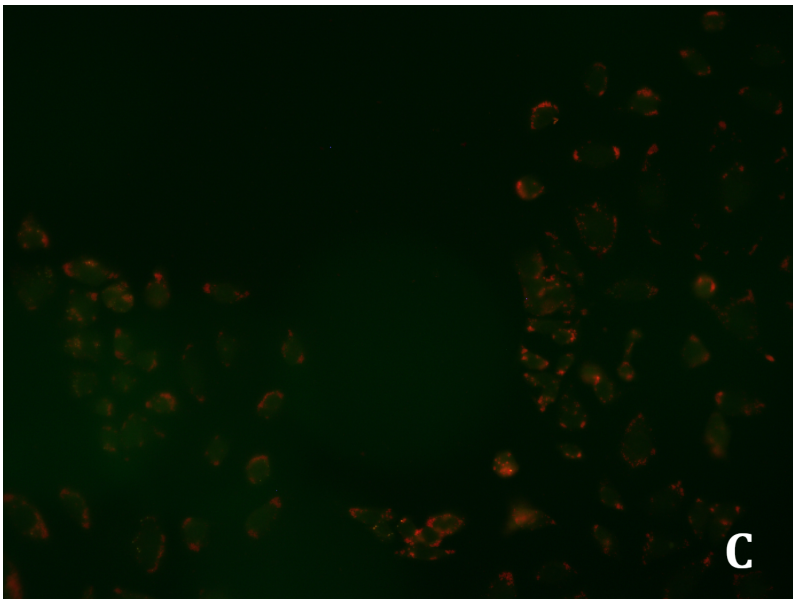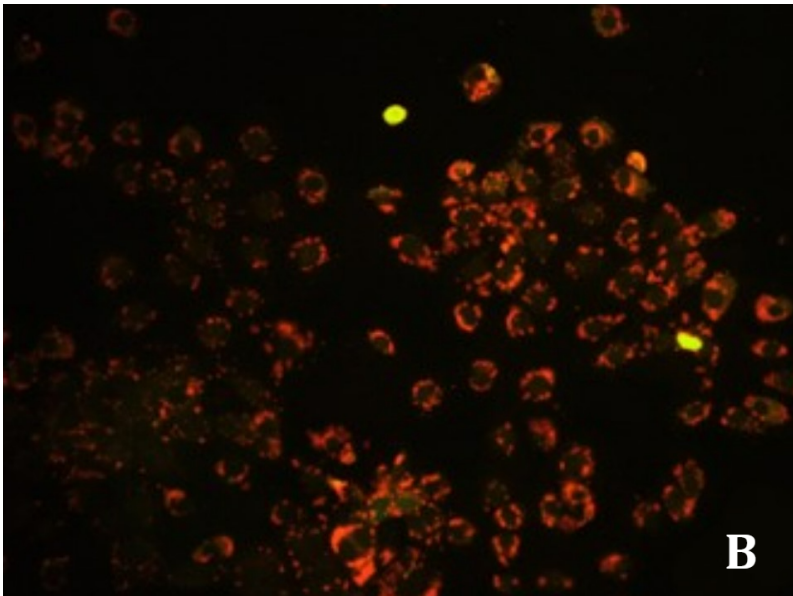
Figure 4: FAT10-infected hepatocytes show higher lipid accumulation after insulin treatment. Fold change measurements from qPCR quantify the relative expression via an unpaired t-test with standard deviation as error bars (A). 200x-magnification of fluorescent images of hepatocytes infected with control lentivirus (B) and FAT10 lentivirus (C) show this qualitatively. Green fluorescence indicates FAT10 expression, and red-orange fluorescence is Oil Red O stain.

Control Lentivirus Standard Curve

$y = 2.889x + 1.1448$
$R^2 = 0.7827$

Absorbance
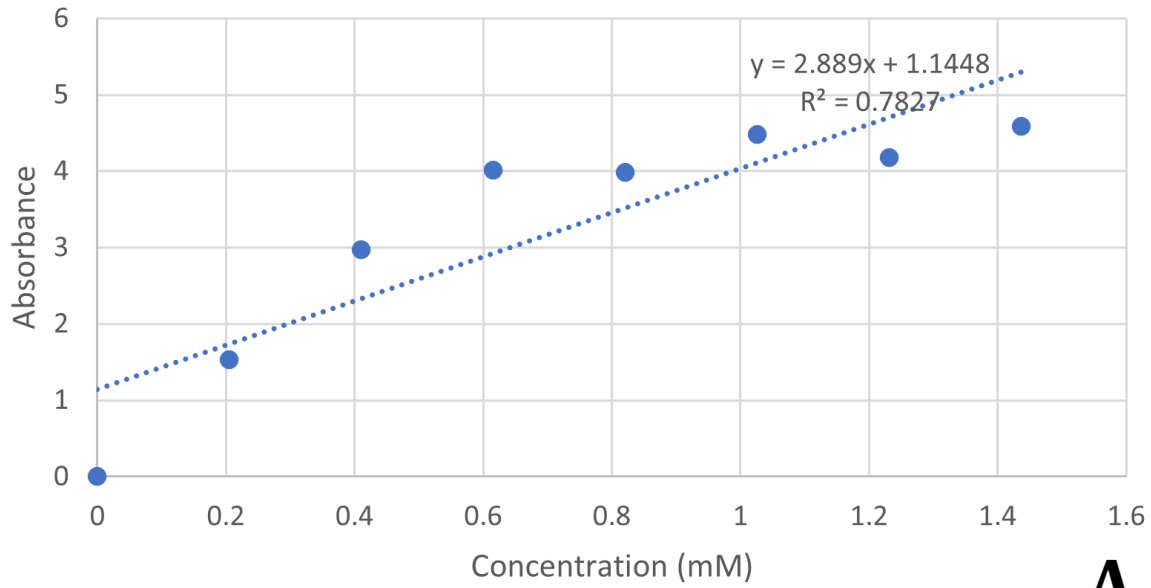
Concentration (mM)

A

FAT10 Lentivirus Standard Curve

$y = 0.3092x + 0.0468$
$R^2 = 0.9022$

Absorbance
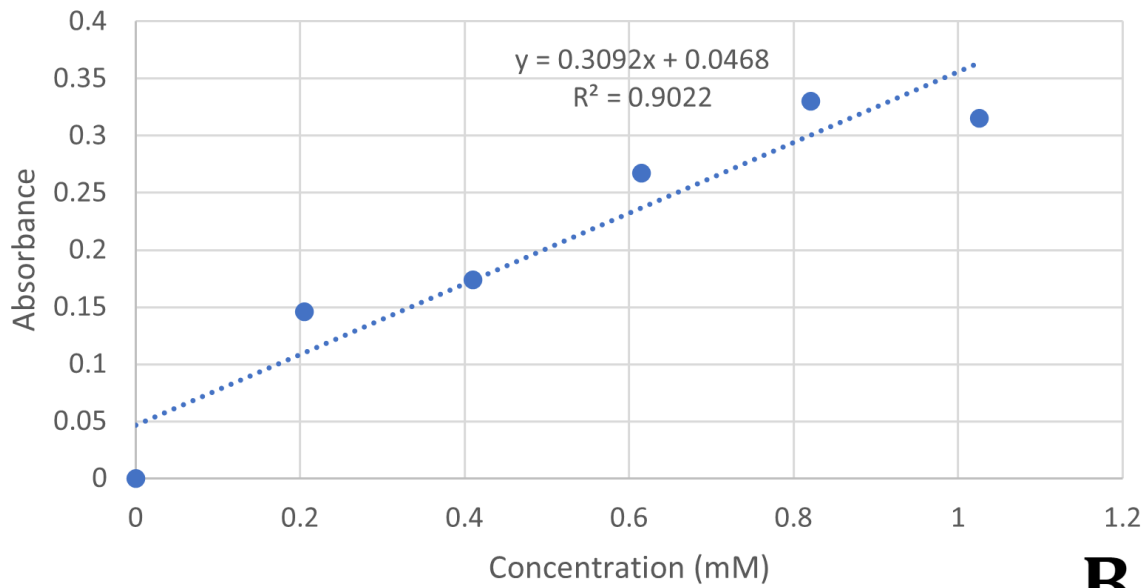
Concentration (mM)

B

Sample Concentration (mM)	
Control Lentivirus	FAT10 Lentivirus
0.250	0.373
0.346	0.505
0.306	0.353
0.315	0.256
0.272	0.638
0.298	**0.425**

Figure 5: UV-vis absorbance at 515 nm confirms higher average lipid retention in FAT10-infected hepatocytes. Standard curves constructed with UV-vis absorbance at 515 nm of ORO in isopropanol (A-B) and sample concentration values for control and FAT10 virus-infected cells (C). The final row in (C) shows the average for each group.

Discussion

The prior study evaluated the use of LEW.1WR1 rats as models for human NASH, via several scoring metrics against Wistar-Furth (WF) rats. These included macro- and microvesicular steatosis (MVS), Mallory-Denk body formation (MDB), and liver inflammation. All these showed significant increases in 1WR1 rats, with particular interest in MVS and MDB.

The former presented as an accumulation of microscopic lipid droplets in the cytoplasm of each hepatocyte, and these were blindly scored for a selection of rat liver slides. Several showed significantly more droplets, and these were later shown to be the modified rats. A similar process was used to evaluate MDB, and likewise produced higher values in 1WR1 rats. The experimental 1WR1 rats showed evidence of hepatocyte damage, obesity and lipid accumulation, and metabolic stress much in line with human symptoms of NAFLD and NASH. Increasing FAT10 activity via viral infection showed markedly more steatosis during *in vitro* studies of hepatocytes in comparison to infection with a control virus. Qualitative and quantitative analyses both showed this result.

Preliminary genetic analysis showed higher expression of FAT10 in 1WR1 rats when evaluating them as human models of NAFLD/NASH, thus prompting these cell-culture studies[4]. These studies together show that not only do 1WR1 rats exhibit human-like NAFLD/NASH with high activity of FAT10, but this higher gene expression is at least one genetic basis for the symptoms of the disease. Medically, this may indicate that gene therapy focused on FAT10/UBD would be more effective than simple treatment of fatty liver.

Some limitations were faced with these *in vitro* experiments. Namely, the FAT10 virus-infected cells were generally less fluorescent than those infected with the control virus, as can be seen in Figure 4. In other words, while more green fluorescence was seen in the former, it was far dimmer, probably due to a lower dose of virus than the latter. It is clear, too, from the same figure that the ORO stain fluoresced in nearly the same range as the green fluorescent protein (GFP) of interest. Moreover, the instrumentation for the UV-vis analysis introduced some complications; the two groups had to be analyzed on different spectrophotometers in order to get values within readable range, thus introducing error between the two. Finally, these experiments were only performed with triplicates of each gene (RPL32 and UBD) for each group, a relatively small number of replicates.

Future experiments will include a stain far outside the range of the GFP, resolving the simultaneous fluorescence of both ORO and GFP. A larger range of standards will solve the issue of UV-vis spectrometry, extending the range of the calibration curve to include all the samples. Using more replicates will make this study far more rigorous overall and absolutely confirm the results. Also, while FAT10 was shown to be a cause for the pathologies of NAFLD and NASH, the exact mechanisms remain unclear and open these pathways to further study.

Conclusion

In total, the results found here show not only that LEW1.WR1 rats have higher instances of cellular damage associated with NAFLD/NASH, but also that these are positively associated with upregulation of the UBD/FAT10 gene. In fact, the higher activity of FAT10 actually serves as a genetic cause for these conditions. Increased FAT10 activity, as shown here, leads to increased microvesicular steatosis, Mallory Denk-body formation, inflammatory body formation, and lipid accumulation in hepatocytes. All of these are significant

markers for NAFLD/NASH in reliable rat models[3]. Understanding these genetic and pathologic mechanisms will allow for better treatment of the diseases in humans, as genetic sequencing in patients could preemptively detect a fatty liver in an otherwise-healthy patient.

Supplemental
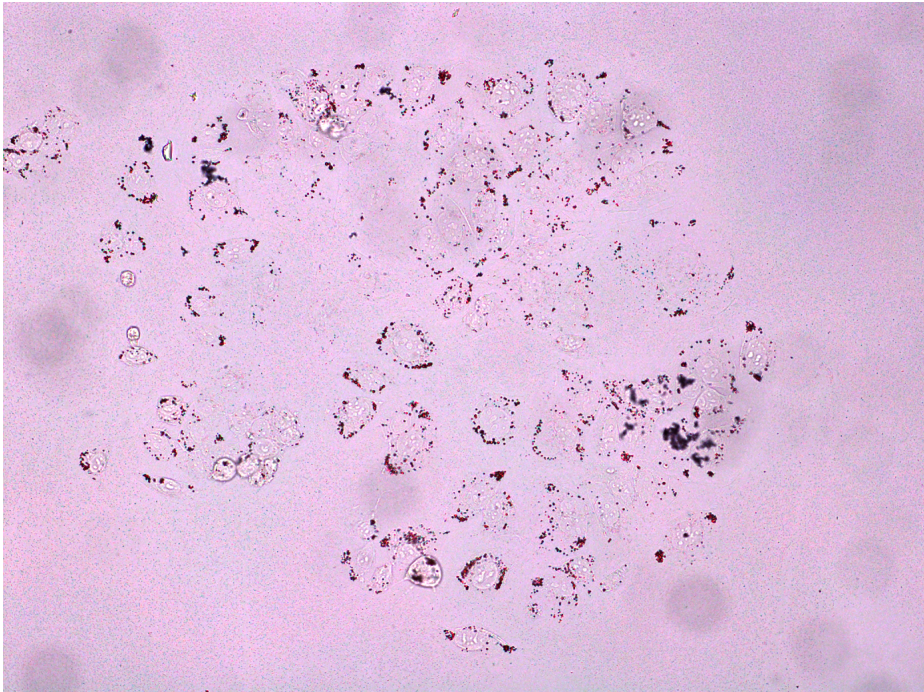
Brightfield microscopy of FAT10 lentivirus cells.

References

(1) Byrne, C. D.; Targher, G. NAFLD: A Multisystem Disease. Journal of

Hepatology 2015, 62 (1), S47–S64. https://doi.org/10.1016/j.jhep.2014.12.012.

(2) Kruger, Annie J., et al. "Haptoglobin as an Early Serum Biomarker of Virus-induced Autoimmune Type 1

Diabetes in Biobreeding Diabetes Resistant and LEW1.WR1 Rats." *Experimental Biology and Medicine*, vol.

235, no. 11, SAGE Publishing, Nov. 2010, pp. 1328–37, doi:10.1258/ebm.2010.010150.

(3) Langford, C.; Goldinger, M. H.; Treanor, D.; McGenity, C.; Dillman, J. R.; Allende, D. S.; Goldin, R. D.;

Brunt, E. M.; Zatloukal, K.; Denk, H.; Fleming, K. A. Improved Pathology Reporting in NAFLD/NASH for

Clinical Trials. Journal of Clinical Pathology 2021, 75 (2), 73–75.

https://doi.org/10.1136/jclinpath-2021-207967.

(4) Love-Rutledge, S.; Wimalarathne, M.; Mercado, L.; Smiley, A.; Apperson, C. R.;

Wilkerson-Vidal, Q. The Type 1 Diabetes Susceptible LEW.1WR1 Rat Develops Insulin

Resistance and Severe Non-Alcoholic Fatty Liver Disease. 2023.

(5) Wree, A.; Broderick, L.; Canbay, A.; Hoffman, H. M.; Feldstein, A. E. From NAFLD to NASH to

Cirrhosis—New Insights into Disease Mechanisms. Nature Reviews Gastroenterology & Hepatology 2013, 10

(11), 627–636. https://doi.org/10.1038/nrgastro.2013.149.